# Dynamic correlations in coupled electron-electron and electron-hole quantum wire systems

L. K. Saini and K. Tankeshwar*
*Department of Physics, Panjab University, Chandigarh - 160 014, India*

R. K. Moudgil†
*Department of Physics, Kurukshetra University, Kurukshetra - 136 119, India*

(Received 12 September 2003; revised manuscript received 23 January 2004; published 10 August 2004)

We investigate theoretically the ground-state behavior of the coupled electron-electron and electron-hole quantum wire systems by incorporating dynamic correlation effects within the quantum version of Singwi, Tosi, Land, and Sjölander theory. The numerical results are presented for the pair-correlation function, the ground-state energy, the static density susceptibility, and the static and dynamic local-field correction factors over a wide range of system parameters, *viz.*, linear particle number density $r_s$, wire size $b$, and interwire spacing $d$. The results reveal that the inclusion of the dynamical nature of particle correlations brings in quantitative as well as qualitative changes in the ground-state behavior of both the electron-electron and electron-hole wire systems. In particular, it is found that these (dynamic) correlations can cause the (homogeneous) liquid phase, in these quantum wire systems, to become unstable against a phase transition into a(n) (inhomogeneous) coupled Wigner crystal ground state at sufficiently low particle density and/or narrow wire size in the close approach of two wires. The interwire correlations are found to reduce the critical $r_s$ for the onset of Wigner crystallization with respect to an isolated quantum wire system, and at $b/a_0^*=1$ the reduction in $r_s$ is about 15% and 4% in the electron-hole and electron-electron wire systems, respectively; $a_0^*$ is the effective Bohr atomic radius. Our prediction of Wigner crystallization for the electron-electron wire system agrees qualitatively with the recent results of Tanatar *et al.*, which they have obtained on the basis of an approximate density functional theory calculation.

DOI: 10.1103/PhysRevB.70.075302 PACS number(s): 73.21.−b, 71.10.−w, 73.20.Qt

## I. INTRODUCTION

Recent years have witnessed a surge of theoretical and experimental studies exploring various static and dynamic properties of the low-dimensional electron systems, where the dynamics of electrons is restricted quantum-mechanically along one or two of the spatial dimensions, thus giving rise to the formation of dynamically two-dimensional (2D)[1] or one-dimensional (1D)[2] electron systems, respectively. These electron systems can be realized, for example, at the interface of semiconductor heterostructures. The development of experimental techniques to grow a periodic structure of such electron systems (the so-called electron superlattice) has added an extra impetus to the importance of their study. Many interesting phenomena have been found[3,4] to arise due entirely to the presence of additional layers of mobile carriers. In particular, Neilson and co-workers,[5] and Kalman *et al.*[6] have theoretically discovered that the interlayer interaction effects can favor a phase transition from the (uniform) liquid state to a (nonuniform) density-modulated ground state, of the charge-density-wave (CDW) and the Wigner crystal (WC) types, in an electron bilayer at sufficiently low electron density in the close vicinity of two layers. Of particular interest is the result that the critical density for the onset of Wigner crystallization is enhanced appreciably in the bilayer as compared to that for an isolated electron layer. This result has been corroborated by the recent quantum Monte Carlo (QMC) simulation studies by Senatore and co-workers.[7] The studies based upon the use of the density functional theory,[8] the mode-coupling approach,[9] and the hypernetted-chain method[10] have also confirmed this result.

In this work, we intend to examine the ground-state behavior of a double quantum wire system, in particular, the stability of its ground state against phase transition into a density-modulated phase of the type as has been predicted[5,6] to occur in an electron bilayer system. In a quantum wire system, the electrons can move freely only along one spatial direction, while their motion is restricted quantum-mechanically along the remaining two transverse directions. These electron systems have attracted considerable attention both from the fundamental and applied physics viewpoints.[2,11] A double quantum wire system consists of two such parallel and spatially separated quantum wires. It is appropriate to mention here that earlier Gold,[12] and Wang and Ruden[13] addressed the problem of the existence of a density-modulated ground state in a double electron quantum wire system, and predicted that this system too could support a CDW ground state at low electron density in the close approach of two wires. Gold predicted the CDW instability in the long-wavelength region (i.e., $q\rightarrow 0$), while Wang and Ruden showed, in addition to the $q\rightarrow 0$ instability, the presence of a CDW instability at $q/q_F=2$ ($q_F$ is the 1D Fermi wave vector). The calculations of Gold, and Wang and Ruden differed in terms of the approximation used for the treatment of intrawire correlations; Gold used the Hubbard approximation,[14] while Wang and Ruden treated these correlations within the self-consistent mean-field approximation of Singwi, Tosi, Land, and Sjölander (STLS),[15] which goes beyond the Hubbard approximation by including the effect of Coulomb correlations. However, the interwire correlations, which may play a vital role when wires are closely placed, were neglected completely in both of these calculations.

 

Moreover, it was assumed that the intrawire correlations are not affected by the interwire interaction effects. Recently, one of the present authors[16] has incorporated both the intra- and interwire correlations on the same footing within the completely self-consistent STLS approach, and found that although the interwire correlations tend to stabilize the liquid phase against transition into a CDW state, their effect is not so strong as to eliminate the existence of a long-wavelength CDW instability.

However, the above investigations did not find any evidence for the WC instability in the double quantum wire system. At this point, we remark that in all of these studies the correlations among carriers are assumed to be static (i.e., time independent), and they appear in the theory in the form of a static local-field correction (LFC) to the bare Coulomb interaction between the carriers. This assumption of treating the correlations as static seems plausible as long as the kinetic effects dominate over the potential energy (i.e., interaction) effects. However, with the increasing departure from this condition, i.e., in the strongly correlated regime, one should anticipate the dynamics of correlations to become increasingly important in determining the many-body properties of the system.[17] This point has recently been demonstrated for the case of an isolated electron layer,[18] and the electron-electron (e-e) and electron-hole (e-h) bilayer systems,[19,20] where the accurate QMC simulations are available[21,22] to compare the theoretical predictions. In view of this, we take into consideration, in our study of the coupled e-e wire system, the dynamical character of both the intra- and interwire correlations. We implement this by employing the dynamic or quantum version[23] of the STLS approach (qSTLS), where the LFC factor is frequency dependent. We also extend our study to the coupled e-h wire system,[24,25] where electrons are replaced by holes in one of the wires. Recently, Tanatar and Bulutay[26] have used the qSTLS method to present a detailed account of various ground-state properties of an isolated electron quantum wire. Moudgil *et al.*[19] have very recently extended the qSTLS approach to the problem of e-e and e-h bilayers, and found that the theory captures reasonably well, though in a qualitative way, the QMC prediction of Wigner crystallization in these systems.

The rest of the paper is organized as follows: In Sec. II, we present the quantum wire model and a brief account of the qSTLS formalism for the double quantum wire system. In Sec. III, we report the numerical results for the various ground-state properties of the coupled e-h and e-e wire systems. The behavior of the static density susceptibility is examined in somewhat more detail to look for any signs of phase transition from the liquid- to a density-modulated phase. The paper is concluded with a brief summary in Sec. IV.

## II. THEORETICAL FORMALISM

### A. Wire model

An electron quantum wire system can be fabricated in laboratory by adding lateral confinement to a 2D electron system. For theoretical studies, this confinement has been modeled in the literature by different confining potentials.[27] In our work, we consider a zero-thickness 2D electron system (say, in the $x$–$y$ plane) and assume the lateral confinement to arise due to the infinite potential barriers at $y=-b/2$ and $b/2$. The particles are assumed to occupy only the lowest energy subbands along the confinement directions. In a double quantum wire system, we have two such parallel wires separated by a center-to-center distance $d(\geqslant b)$. With these assumptions, the wave functions of the particles in two wires do not overlap; therefore, the tunneling of particles between two wires can be ignored in our model. The carriers are electrons in one wire and electrons or holes in the other for the e-e and e-h wire systems, respectively. The wires are assumed to be identical in each respect except for the charge of carriers in the e-h wire system. Further, the wire system is assumed to be embedded in a uniform charge neutralizing background to maintain the charge neutrality. Ignoring the effect of averaging over the finite extent of the carrier wave function in the lateral direction, the Coulomb interaction potential among carriers is obtained as

$$V_{ll'}(q) = \alpha_{ll'}\frac{2e^2}{\epsilon_0}K_0(q\sqrt{b^2+|l-l'|d^2}), \tag{1}$$

with $l=1,2$ the wire index, $\alpha_{ll'}=1$ and $(-1)^{|(l-l')|}$ for the e-e and e-h wires, respectively, $\epsilon_0$ the dielectric constant of the background wire material, and $K_0(x)$ the zeroth-order modified Bessel function of the first kind. Apparently, the ground state of the above wire model will depend, apart from the particle number density $n$, on the interwire spacing $d$ and the wire diameter $b$. The particle density is usually expressed in terms of a dimensionless parameter $r_s=1/(2na_0^*)$, where $a_0^*=\epsilon_0\hbar^2/(m^*e^2)$ is the effective Bohr atomic radius, with $m^*$ being the effective mass.

### B. Theory

We use the dielectric formulation, developed in the linear response framework, as the theoretical procedure. In this approach, the wave vector and frequency-dependent density-density response function, $\chi(q,\omega)$, plays a central role as it contains the necessary information about the relevant static and dynamic properties of the system. For the double wire system, the qSTLS derivation of $\chi(q,\omega)$ proceeds exactly analogous to the one for the bilayer system given in Ref. 19, except for the basic fact that the 2D variables are now replaced with the 1D ones. Therefore, we give in the following only the central relations of the qSTLS derivation for $\chi(q,\omega)$.

The density-density response function for the double wire system can be compactly expressed in the form of a $2\times 2$ matrix, with the elements of the inverse of the density response matrix given by

$$\chi_{ll'}^{-1}(q,\omega) = \frac{\delta_{ll'}}{\chi_l^0(q,\omega)} - V_{ll'}(q)[1-G_{ll'}(q,\omega)], \tag{2}$$

where $\chi_l^0(q,\omega)$ is the zero-temperature density response function of the noninteracting electrons in wire $l$ (i.e., the 1D Stern function[28]), and

$$G_{ll'}(q,\omega) = -\frac{1}{n}\int_{-\infty}^{\infty}\frac{d\mathbf{q}'}{2\pi}\frac{\chi_l^0(\mathbf{q},\mathbf{q}';\omega)}{\chi_l^0(\mathbf{q},\omega)}\frac{V_{ll'}(q')}{V_{ll'}(q)} \times[S_{ll'}(|\mathbf{q}-\mathbf{q}'|)-\delta_{ll'}], \tag{3}$$

is the *dynamic* LFC factor that accounts for the short-range correlation effects among carriers in the wires $l$ and $l'$. In the above equation, $S_{ll'}(q)$ is the static density structure factor and $\chi_l^0(\mathbf{q},\mathbf{q}';\omega)$ the inhomogeneous Stern function given by

$$\chi_l^0(\mathbf{q},\mathbf{q}';\omega) = -\frac{2}{\hbar}\int_{-\infty}^{\infty}\frac{d\mathbf{k}}{2\pi}\frac{f_l^0(\mathbf{k}+\mathbf{q}'/2)-f_l^0(\mathbf{k}-\mathbf{q}'/2)}{\omega-\hbar kq/m+\iota\eta}, \tag{4}$$

where $f_l^0(\mathbf{k})$ is the noninteracting Fermi-Dirac distribution function and $\eta$ is a positive infinitesimal. For $\mathbf{q}'=\mathbf{q}$, $\chi_l^0(\mathbf{q},\mathbf{q}';\omega)$ reduces to the homogeneous Stern function $\chi_l^0(q,\omega)$.

The fluctuation-dissipation theorem, which relates the static structure factor with the imaginary part of the linear response function as

$$S_{ll'}(q) = -\frac{\hbar}{n\pi}\int_0^{\infty} d\omega\ \mathrm{Im}\ \chi_{ll'}(q,\omega), \tag{5}$$

closes the qSTLS set of equations for the density response matrix. Apparently, these equations are to be solved numerically in a self-consistent manner for the calculation of the response function.

The pair-correlation function $g_{ll'}(r)$, which defines the probability of finding a particle in wire $l'$ at a parallel distance of $r$ given that there is a particle at origin in wire $l$, can be obtained directly from the inverse Fourier transform of the static structure factor as

$$g_{ll'}(r) = 1+\frac{1}{n}\int_{-\infty}^{\infty}\frac{d\mathbf{q}}{2\pi}\cos(qr)[S_{ll'}(q)-\delta_{ll'}]. \tag{6}$$

The ground-state energy $E_{gs}$ can also be determined from the knowledge of the static structure factor by a straightforward extension of the ground-state energy theorem[29] to the two-wire system as

$$E_{gs} = E_0+\int_0^{e^2}\frac{d\lambda}{\lambda}E^{\mathrm{int}}(\lambda), \tag{7}$$

where $E_0=p_F^2/(6m^*)$ is the kinetic energy per particle of the noninteracting system ($p_F=\hbar q_F$ is the 1D Fermi momentum), $\lambda$ is the strength of the Coulomb interaction potential, and $E^{\mathrm{int}}(\lambda)$ is the interaction energy per particle, given by

$$E^{\mathrm{int}}(\lambda) = \frac{1}{4}\sum_{l,l'}^{2}\int_{-\infty}^{\infty}\frac{d\mathbf{q}}{2\pi}\lambda V_{ll'}(q)[S_{ll'}(q;\lambda)-\delta_{ll'}]. \tag{8}$$

It is appropriate to point out here that the LFCs, which enter into the density response calculation [(Eq. (2)], are frequency independent (i.e., static) in the STLS approach, and these formally correspond to setting $\chi_l^0(\mathbf{q},\mathbf{q}';\omega) = (qq'/q)\chi_l^0(q,\omega)$ in Eq. (3). Technically, the basic difference between the quantum and the original STLS methods lies in the fact that one seeks in the former the solution of the quantum-mechanical equation of motion for the quantum single-particle distribution function, namely, the Wigner distribution function (WDF), and this equation is just the quantum analog of the corresponding classical equation of motion for the classical distribution function used in the original STLS approach. Nevertheless, the quantum approach employs exactly the same decoupling approximation as that of the original STLS method to truncate the infinite hierarchy of the coupled equations of motion; the two-particle WDF is approximated as a product of the respective single-particle WDFs and the equilibrium static pair-correlation function. Thus, the dynamical nature of the qSTLS LFCs should be seen as a quantum-mechanical correction to the original STLS approach. The dynamics of spatial correlations among carriers, which is expected to become vital at relatively higher values of Coulomb coupling (i.e., at higher $r_s$), is still missing.

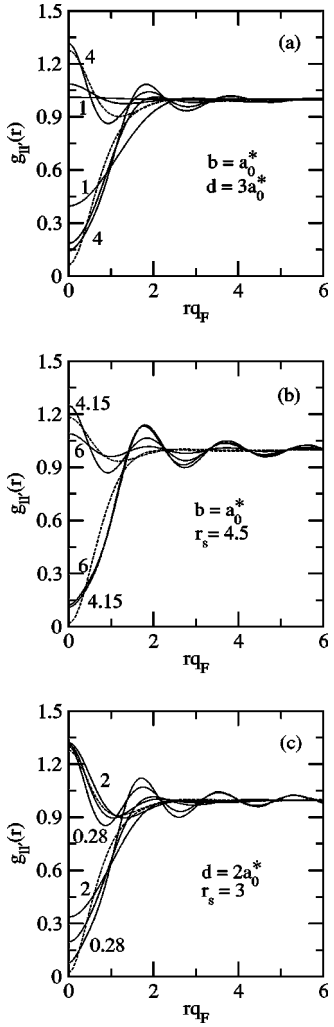


FIG. 1. Pair-correlation functions $g_{11}(r)$ and $g_{12}(r)$, commencing, respectively, in the lower and upper halves of the figure, for the e-h wire system in the qSTLS (solid lines) approach at: (a) $r_s=1,2.5$, and 4; (b) $d/a_0^*=6$ and 4.15; and (c) $b/a_0^*=2,1$, and 0.28 at indicated wire parameters. The STLS results (dashed lines) are at: (a) $r_s=4$; (b) $d/a_0^*=4.15$; and (c) $b/a_0^*=0.28$.

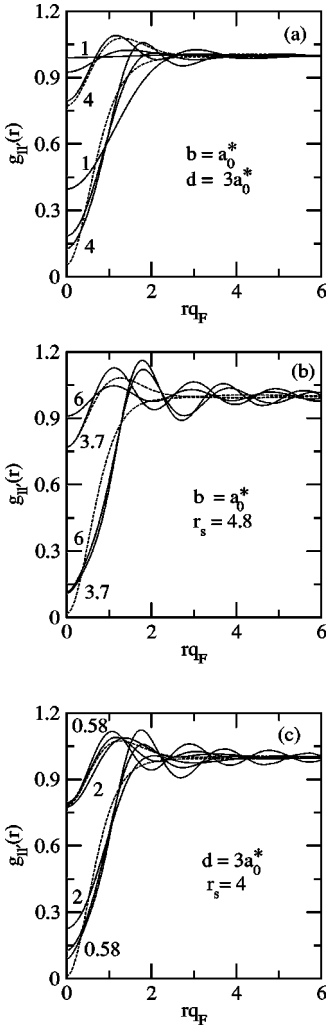


FIG. 2. Pair-correlation functions $g_{11}(r)$ and $g_{12}(r)$, commencing, respectively, in the lower and upper halves of the figure, for the e-e wire system in the qSTLS (solid lines) approach at: (a) $r_s=1,2.5$, and 4; (b) $d/a_0^*=6$ and 3.7; and (c) $b/a_0^*=2,1$, and 0.58 at indicated wire parameters. The STLS results (dashed lines) are at: (a) $r_s=4$; (b) $d/a_0^*=3.7$; and (c) $b/a_0^*=0.58$.

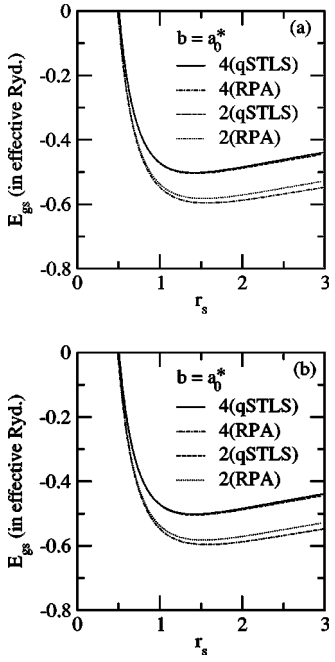


FIG. 3. Comparison of ground-state energy (per particle) $E_{gs}$ between the qSTLS and RPA approaches for the coupled e-h [in panel (a)] and e-e [in panel (b)] wire systems at $d/a_0^*=4$ and 2; legends indicate the values of $d/a_0^*$.

In the following section, we present numerical results for the various ground-state properties of the e-h and e-e wire systems.

## III. RESULTS AND DISCUSSION

### A. Pair-correlation functions

Equations (2), (3), and (5) are solved numerically in a self-consistent manner for the static structure factor $S_{ll'}(q)$. The $\omega$ integration in the numerical computation of $S_{ll'}(q)$ [Eq. (5)] is performed along the imaginary $\omega$ axis in order to avoid the problem of dealing with the plasmon poles which appear on the real $\omega$ axis (see de Freitas *et al.*[30] and Ref. 18). We accepted the self-consistent solution when convergence in results of $S_{ll'}(q)$ (at each $q$ in the grid of $q$ points) was better than $10^{-7}$. We report here, in place of $S_{ll'}(q)$, the results for the pair-correlation function $g_{ll'}(r)$, as it contains rather direct information about correlations among particles. It is appropriate to mention here that in all of our numerical calculations we have assumed the effective mass of holes to be equal to that of electrons (i.e., $m_h^*=m_e^*$).

We show in Figs. 1(a)–1(c) the results for the intra- and interwire pair-correlation functions, $g_{11}(r)$ and $g_{12}(r)$, over a wide range of system parameters (*viz.*, the particle density $r_s$, the wire spacing $d$, and the wire diameter $b$) for the e-h wire system. For ready comparison, the corresponding STLS curves are also given in the same figures at some selected wire parameters. Figure 1(a) depicts the $r_s$ dependence of $g_{11}(r)$ and $g_{12}(r)$ at fixed $b$ and $d$. It is apparent that both the intra- and interwire correlations grow in their strength with increasing $r_s$ (i.e., decreasing density) and they exhibit an oscillatory behavior for $r_s \geqslant 2$, with the amplitude of oscillations being an increasing function of $r_s$. The oscillatory behavior becomes quite appreciable for $r_s \geqslant 4$. In Fig. 1(b), $g_{11}(r)$ and $g_{12}(r)$ are shown at different values of $d$ by keeping $r_s$ and $b$ as fixed parameters. Clearly, $g_{11}(r)$ depends only weakly on $d$, while $g_{12}(r)$ shows a noticeable growth in its magnitude with decreasing $d$.

As the wire size $b$ appears directly in the expression of interaction potential [Eq. (1)], it may possibly be used as an alternative (i.e., in addition to $r_s$ and $d$) experimental parameter to probe the behavior of the wire system in different correlation regimes. It is, therefore, interesting to examine here the behavior of $g_{11}(r)$ and $g_{12}(r)$ as a function of $b$, and the same is reported in Fig. 1(c) by treating $r_s$ and $d$ as fixed parameters. A cross comparison of Figs. 1(a)–1(c) clearly reveals that one can afford to have a strongly correlated regime at a rather low $r_s$ value by reducing the wire size $b$. Also, we find from the comparison between the qSTLS and

STLS results that at low $r_s(\leqslant 1)$ there is little difference in the predictions of the two approaches; therefore, the STLS results are not shown at these $r_s$ values. However, the difference starts building up with increasing $r_s$ and as a distinctive feature the STLS approach, in contrast with the qSTLS results, does not predict any kind of oscillatory behavior for the pair-correlation functions.

Figures 2(a)–2(c) present our results of $g_{11}(r)$ and $g_{12}(r)$ for the e-e wire system at different wire parameters, along with the STLS results at some selected wire parameters. We notice that $g_{11}(r)$ and $g_{12}(r)$ for the e-e system exhibit at the qualitative level a similar dependence on $r_s$, $d$, and $b$ as that for the e-h system, except for the primary difference that the interwire correlations are now of repulsive nature.

### B. Ground-state energy

The self-consistently obtained static structure factors $S_{11}(q;\lambda)$ and $S_{12}(q;\lambda)$ are used in Eq. (8) to calculate $E^{\rm int}(\lambda)$ as a function of $\lambda$. The ground-state energy is then determined by performing the coupling-constant (i.e., $\lambda$) integration in Eq. (7). The numerical results of ground-state energy (per particle) for the e-h and e-e wire systems are given, respectively, in Figs. 3(a) and 3(b) as a function of $r_s$ for $d/a_0^*=4$ and 2 at $b/a_0^*=1$. It can be noticed that the ground-state energy depends only weakly on the wire separation. Also, we check that in the limit of large separation between wires our results approach the results of an isolated wire. This is expected as the interwire interactions become very small in the large-$d$ limit. To highlight the role of correlations, we have compared our results with those obtained in the random phase approximation (RPA), where correlations among particles are completely ignored. It may be noted that the exclusion of correlations leads to an overestimation of ground-state energy. Further, there is a very small difference between the qSTLS and STLS results; the STLS curves are, therefore, not given here.

### C. Density-modulated ground state

In this section, we address the main question of whether a double quantum wire system can support a phase transition from the (homogeneous) liquid state to a(n) (inhomogeneous) density-modulated ground state of the type as has been predicted to occur in a bilayer system.[5,19] For this purpose, we examine, parallel to the bilayer problem,[19] the behavior of the liquid-state static (i.e., $\omega=0$) density susceptibility as a function of wire parameters. Diagonalizing the density response matrix (2), the static density susceptibility is obtained as

$$\chi_{\pm}(q,0)=\frac{\chi_1^0(q,0)}{1-\chi_1^0(q,0)[V_{11}(q)(1-G_{11}(q,0))\pm V_{12}(q)(1-G_{12}(q,0))]}. \tag{9}$$

The + and − signs correspond, respectively, to the in-phase and out-of-phase ($\pi$) modes of density modulations in two wires. $\chi_1^0(q,0)$ $(=\chi_2^0(q,0))$ is the static 1D Stern function. The presence of a phase transition to a density-modulated state (if any) may appear as a divergence in $\chi_{\pm}(q,0)$ at a wave vector value corresponding to the reciprocal lattice vector associated with the density-modulated state. We, therefore, look for poles of Eq. (9). However, this can only be achieved numerically in our approach, since the intra- and interwire LFCs, which appear in the denominator of Eq. (9), can only be determined in a numerical way from the self-consistent solution of Eqs. (2), (3), and (5). But, it is evident from Eq. (9) that these are the in-phase and out-of-phase components of the susceptibility which can have a divergence in the e-h and e-e wire systems, respectively. Also, since the e-h and e-e correlations are of opposite nature, they should tend, respectively, to support and oppose a phase transition to a density-modulated phase (if any) in the e-h and e-e wire systems. We first discuss the behavior of the e-h wire system.

#### *1. Coupled electron-hole wires*

Figures 4(a)–4(d) show the results of $\chi_+(q,0)$ at some selected values of $r_s$ and $d$ for $b/a_0^*=1$. For low $r_s(\leqslant 1)$ values, $\chi_+(q,0)$ is found to exhibit a single sharp peak at $q/q_F=2$ [Fig. 4(a)], with the peak height increasing gradually on decreasing $d$, but its value remaining finite for the range of $d$ values allowed in our model (i.e., $d\geqslant b$). At $r_s=2$ too, there is no singularity found in $\chi_+(q,0)$, but an additional peak starts developing at small $q$, and the large-$q$ peak (i.e., the one at $q/q_F=2$ for $r_s=1$) moves slightly to its higher side on the $q$ axis. With further increase in $r_s$, the peak at small $q$ becomes quite dominant in its strength over the peak positioned at $q/q_F>2$. This can be noticed from Fig. 4(b), where $\chi_+(q,0)$ is plotted at $r_s=3$; $d/a_0^*=2, 1.8$, and 1.75. We notice that the small-$q$ peak grows quite fast in its height with decreasing $d$. However, we encounter now a critical wire spacing $d_c$ below which it becomes almost impossible to obtain the self-consistent solution of Eqs. (2), (3), and (5) and, hence, the $\chi_+(q,0)$; for instance, $d_c/a_0^*\approx 1.75$ at $r_s=3$ and $b/a_0^*=1$. As has been the case for the bilayer problem,[19] the difficulty in obtaining the self-consistent solution emanates due to the appearance of a numerical instability in the density response function while computing $S_{ll'}(q)$ from Eq. (5). Although we are not able here to calculate $\chi_+(q,0)$ for $d<d_c$, the peak at small $q$ appears to diverge in this $d$ region. The small-$q$ peak continues to dominate over the large-$q$ peak until a critical value of $r_s$ is reached, at which point the large-$q$ peak starts dominating. At $b/a_0^*=1$,

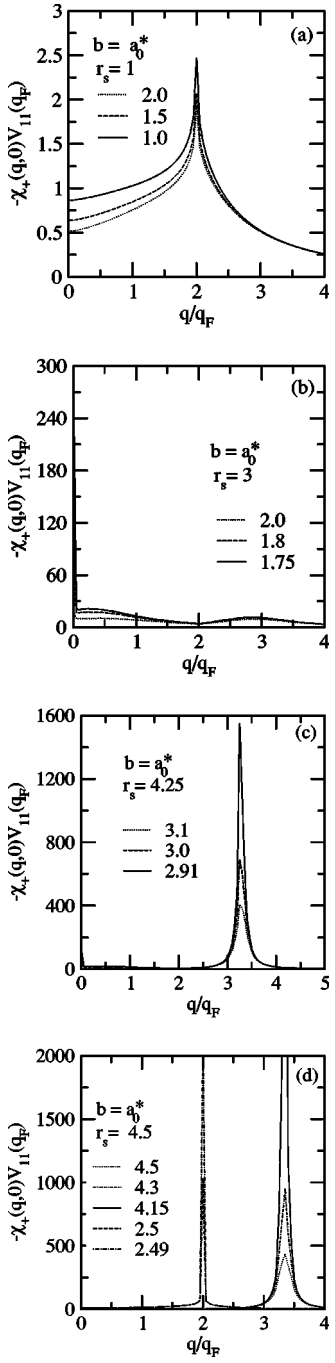


FIG. 4. (a)–(d) In-phase component of the static density susceptibility $\chi_+(q,0)$ for the coupled e-h wire system for different $d/a_0^*$ at indicated $r_s$ and $b/a_0^*$, according to the qSTLS theory. For comparison, the STLS results are given in (d) at $d/a_0^*=2.5$ and 2.49. Legends indicate the values of $d/a_0^*$.

this shift occurs at $r_s \approx 4.25$. This point is demonstrated in Fig. 4(c), where $\chi_+(q,0)$ is plotted at $r_s=4.25$ and $d/a_0^*=3.1, 3$, and 2.91; here, $d_c/a_0^* \approx 2.91$. The large-$q$ peak is now positioned at $q/q_F \approx 3.4$. Increasing $r_s$ beyond 4.25 results in a complete disappearance of the small-$q$ peak, with the large-$q$ peak continuing to appear at $q/q_F \approx 3.4$, as can be noticed from Fig. 4(d) where $\chi_+(q,0)$ is shown at $r_s=4.5$ and $d/a_0^*=4.5, 4.3$, and 4.15; $d_c/a_0^* \approx 4.15$.

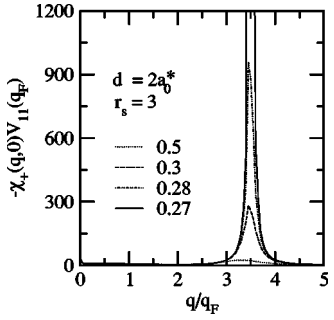


FIG. 5. In-phase component of the static density susceptibility $\chi_+(q,0)$ for the coupled e-h wire system for different $b/a_0^*$ at indicated $r_s$ and $d/a_0^*$, according to the qSTLS approach; legends indicate the values of $b/a_0^*$.

As in the bilayer problem,[19] the development of a strong and seemingly diverging peak in $\chi_+(q,0)$ at small $q$ could be interpreted as a precursor for the instability of the liquid state in the e-h wire system against transition into a (long-wavelength) CDW ground state. Meanwhile, the $q/q_F \approx 3.4$ peak, whose position lies close to the reciprocal lattice vector ($q/q_F=4$) of a linear lattice, could indicate the instability of the liquid phase against transition into a coupled WC ground state. This interpretation is supported if we look at the behavior of the pair-correlation functions as given in Fig. 1(b) at $r_s=4.5$ and $d/a_0^*=6$ and 4.15. Evidently, $g_{11}(r)$ and $g_{12}(r)$ exhibit pronounced in-phase oscillations at $d/a_0^*=4.15$, signaling a strong tendency for the formation of an ordered WC phase in the e-h wire system. Although not reported here, the static structure factor $S_{11}(q)$ shows for $r_s \geqslant 4.25$ a strong maxima at a wave vector value coinciding almost exactly with the position of the large-$q$ peak in $\chi_+(q,0)$, which provides further support to our claim for the onset of transition to the WC phase.

Thus, a crossover seems to occur from a CDW ground state to a WC ground state at a critical density $r_s^c \approx 4.25$. We have also performed the qSTLS calculations of the static density susceptibility for an isolated electron quantum wire. It is found that this system too can become unstable against transition to an ordered WC phase, and at $b/a_0^*=1$ the critical density is $r_s \approx 5$. However, there is no indication for the existence of a CDW phase. Thus, we may deduce that the e-h correlations in the e-h wire system act to lower the critical $r_s$ for Wigner crystallization as compared to that for an isolated quantum wire, and at $b/a_0^*=1$, the reduction in $r_s$ is about 15%.

Further, we have also examined the behavior of $\chi_+(q,0)$ as a function of $b$, in particular, its role in determining the critical density for the onset of Wigner crystallization. In Fig. 5 we depict $\chi_+(q,0)$ at $r_s=3$ and $d/a_0^*=2$ as a function of decreasing $b$. It may be noted from Fig. 4(b) that the small-$q$ peak is relatively stronger than the one at large $q$ at $b/a_0^*=1$. However, with reduction in $b$, the large-$q$ peak grows monotonically (Fig. 5) in its magnitude, with its position moving gradually towards higher $q$ on the $q$ axis. The large-$q$ peak is eventually seen to dominate over the small-$q$ peak for $b/a_0^* \leqslant 0.5$. A critical value of $b$ ($\approx 0.27 a_0^*$) is encountered, below which it becomes impossible to obtain a self-

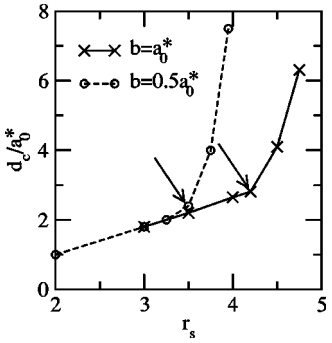


FIG. 6. Critical wire spacing $d_c/a_0^*$ depicting the points of instability for the coupled e-h wire system as a function of $r_s$ at $b/a_0^*=1$ and 0.5. The lines are just a guide for the eye. For each case the arrows show the critical $r_s$ where crossover from the CDW instability to the Wigner crystal instability occurs.

consistent solution of the qSTLS equations, which can again be interpreted as a signature for transition into a density-modulated phase. At $b/a_0^*=0.27$, the peak in $\chi_+(q,0)$ is located at $q/q_F\approx 3.5$. This leads us to recognize the emerging density-modulated phase as of the WC type. More physical insight can be gained from the knowledge of the corresponding $b$ dependence of $g_{11}(r)$ and $g_{12}(r)$, which has been displayed already in Fig. 1(c). Clearly, the behavior of the correlation functions is quite similar to the one at $r_s=4.5$ and $b/a_0^*=1$ [Fig. 1(b)]. It may be recalled here that the CDW phase dominated at $b/a_0^*=1$ for $r_s$ approximately up to 4.2. In view of this result, we may conclude that the critical $r_s$ for the onset of Wigner crystallization can be reduced by reducing the wire size $b$. Further, at a given $r_s$, the critical $b$ for the onset of WC phase is found to increase with decreasing $d$. One can obtain, at the cost of computation time, a phase diagram in the $r_s-d-b$ space depicting the regions of stability of the liquid- and the density-modulated phases, respectively. For example, we have plotted in Fig. 6 the critical wire spacing $d_c/a_0^*$ as a function of $r_s$ at $b/a_0^*=1$ and 0.5. It may be noted that a reduction in $b$ lowers the cutoff $r_s$ for the onset of instability, while it results in an increase in $d_c$ at a given $r_s$. Also, the critical $r_s$ at which a crossover from a CDW state to a WC state occurs decreases with a decrease in $b$.

It is interesting to compare our above prediction on the existence of a density-modulated phase with the corresponding results obtained by using the STLS approach. We find that the STLS calculations of $\chi_+(q,0)$ also signal a transition into a density-modulated phase, but only of the CDW type, with $q/q_F=2$ as the CDW wave vector. There is no evidence found for transition into a WC ground state. For comparison, the STLS $\chi_+(q,0)$ is plotted in Fig. 4(d) at $r_s=4.5$, $b/a_0^*=1$, and $d/a_0^*=2.5$ and 2.49. We should mention here that Thakur and Neilson[25] have previously studied the e-h wire system within the STLS approach by including the mass asymmetry of the system (i.e., $m_h^*\neq m_e^*$), and detected an instability of the CDW type only.

In order to understand the above difference between the predictions of the qSTLS and STLS approaches, we draw a comparison between their respective intra- and interwire LFCs, since the behavior of $\chi_\pm(q,0)$ [Eq. (9)] is solely determined in terms of these LFCs. Figures 7(a) and 7(b) show, respectively, the static (i.e., $\omega=0$) qSTLS intra- and interwire LFCs along with the STLS LFCs (which, of course, are originally static) at $r_s=4.5$, $b/a_0^*=1$, and different values of $d/a_0^*$. We notice a marked difference in the results of the two approaches. Among the notable distinctive points, $G_{11}(q,0)$ and $G_{12}(q,0)$ exhibit an oscillatory behavior as a function of $q$, with their values becoming exactly equal to zero at $q/q_F=2$. $G_{11}(q,0)$ has a sharp maximum at $q/q_F\approx 4$, with its value lying well above unity. The zero at $q/q_F=2$ in $G_{11}(q,0)$ and $G_{12}(q,0)$ arises due to the fact that $\chi^0(q,0)$, which appears directly in the denominator of $G_{ll'}(q,0)$ [Eq. (3)], has logarithmic singularity at $q/q_F=2$. On the other hand, the STLS LFCs depend quite smoothly on $q$ and in particular, $G_{11}(q)$ hardly exceeds unity in the relevant $q$ region. It may be noted here that $\chi(q,0)$ for the single wire system can exhibit a singular behavior only if the corresponding LFC factor exceeds unity by a sufficient amount. However, this is not seen to be a necessary condition for the double wire system due to the presence of the interwire interaction term in the denominator of Eq. (9), i.e., $\chi_\pm(q,0)$ can exhibit singularity at some $q$ even if the single wire $\chi(q,0)$ is a nonsingular one. Now, the behavior of the single wire static LFC factor is found, both in the STLS and qSTLS approaches, to be qualitatively similar to that of the intrawire LFC of the double wire system. As a result, the single wire STLS $\chi(q,0)$ does not show any divergence in the investigated density range of $r_s\leqslant 25$ for $b/a_0^*=1$, while the qSTLS $\chi(q,0)$ appears to diverge clearly at $r_s\approx 5$ for $b/a_0^*=1$, with its peak located at $q/q_F\approx 3.4$. Thus, in the qSTLS approach, the e-h interaction term tends to reduce the critical $r_s$ value

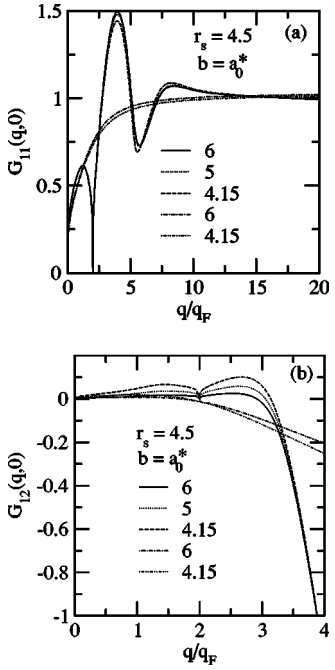


FIG. 7. Intrawire [in panel (a)] and interwire [in panel (b)] static local fields $G_{11}(q,0)$ and $G_{12}(q,0)$ for the coupled e-h wire system in the qSTLS approach at indicated $r_s$, $b$, and $d$. The STLS local fields are shown for comparison at $d/a_0^*=6$ and 4.15. Legends indicate the values of $d/a_0^*$.

for the onset of divergence in the $q/q_F \approx 3.4$ peak in $\chi_+(q,0)$, and to give rise to an additional diverging peak in $\chi_+(q,0)$ (in the close approach of wires) at small $q$ for $r_s$ greater than a certain cutoff value, but lower than the critical $r_s$ for the dominance of $q/q_F \approx 3.4$ peak. In the STLS approach, the e-h interactions give rise to only a single diverging peak in $\chi_+(q,0)$ at $q/q_F \approx 2$ for $r_s$ greater than a certain cutoff value. Therefore, the origin of the $q/q_F \approx 3.4$ peak in $\chi_+(q,0)$, whose divergence in our approach has been interpreted as a signature of transition into an in-phase coupled WC state in view of the proximity of its location to the reciprocal lattice vector of the linear lattice and the behavior of corresponding pair-correlation functions, may be explicitly attributed to the inclusion of the dynamical nature of correlations in the form of the dynamic qSTLS LFC factors.

Further, we may note that in the $q$ region where the static LFC factor $G(q,0)$ exceeds unity, the effective static interaction $[V(q)(1-G(q,0))]$ becomes negative (i.e., attractive), and may give rise to the superconducting pairing[31] in the system. Apart from this, the attractive e-h correlations in the e-h system may also lead to the formation of bound e-h pairs (excitons) in the sufficiently close approach of two wires, as has been predicted recently for an e-h bilayer system[22] by the QMC simulations. The possibility of the superconducting and the excitonic instabilities, and in particular, their role with respect to the predicted existence of the WC instability, can possibly be better examined on the basis of the total energy calculations of the respective phases of the system; this seems to be beyond the scope of our present theoretical approach.

#### *2. Coupled electron-electron wires*

Here, our interest lies in the behavior of the out-of-phase component of the static susceptibility, i.e., $\chi_-(q,0)$. We infer from a careful analysis of our results of $\chi_-(q,0)$ that, although the interwire correlations in the e-e system have the tendency to suppress the peak-like structure in $\chi_-(q,0)$, these are not sufficiently strong in their effect so as to preclude the possibility of transition to a density-modulated phase. Our results of $\chi_-(q,0)$ are plotted in Figs. 8(a)–8(c) at $b/a_0^*=1$, and different $r_s$ and $d$ values of interest. $\chi_-(q,0)$ does not show any singular behavior at low $r_s(\leqslant 2)$ values. A long-wavelength CDW instability appears at $r_s \approx 3$, which now continues to dominate completely for $r_s$ up to 4.7. However, there emerges an interesting and peculiar behavior of $\chi_-(q,0)$ at $r_s=4.8$ as can be noticed from Fig. 8(c). $\chi_-(q,0)$ exhibits a single strong peak at $q/q_F \approx 3.3$ when the wires are widely separated. The peak height initially increases with decrease in $d$, seems to diverge at $d/a_0^* \approx 4.8$, then starts decreasing monotonically with further decrease in $d$. For $d/a_0^* < 4.5$, there starts developing, however, a second peak in $\chi_-(q,0)$ at small $q$, with its magnitude growing continuously relative to that of the large-$q$ peak on decreasing $d$. Eventually, the small-$q$ peak is found to dominate for $d/a_0^* \leqslant 3.7$. This might imply that there is a crossover to the WC ground state at $r_s \approx 4.8$, with the WC state, however, remaining stable only over a certain range of wire spacing, with a transition back to the long-wavelength CDW phase when the wire spacing is further diminished. Parallel to the the e-h wire system, the critical $r_s$ for Wigner crystallization is found to depend upon the wire size $b$. For example, the WC ground state could be stable at $r_s=4$ and $d/a_0^*=3$ by reducing the wire size $b/a_0^*$ approximately to 0.58 (Fig. 9). We may recall here that it was the CDW phase which was seen to be stable at $r_s=4$ and $b/a_0^*=1$ [see Fig. 8(b)]. It may also be noted from Figs. 2(b) and 2(c) that $g_{11}(r)$ and $g_{12}(r)$ show a noticeable oscillatory behavior, typical of an ordered phase, at wire parameters associated with the onset of Wigner crystallization.

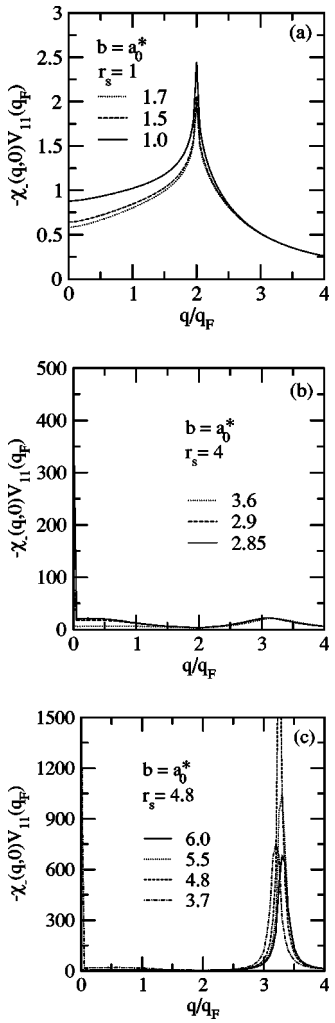


FIG. 8. (a)–(c) Out-of-phase component of the static density susceptibility $\chi_-(q,0)$ for the coupled e-e wire system in the qSTLS approach for different $d/a_0^*$ at indicated $r_s$ and $b/a_0^*$; legends indicate the values of $d/a_0^*$.

Thus, the interwire correlations in the e-e wire system act to reduce (by about 4% at $b/a_0^*=1$) the critical $r_s$ for Wigner crystallization with respect to an isolated electron quantum wire. The reduction in critical $r_s$ is, however, smaller as compared to that found for the e-h wire system. Our prediction of Wigner crystallization in the e-e wire system agrees qualitatively with the recent results of Tanatar, [32] where the authors have examined the problem of freezing within the density functional theory. Their approximate total energy calcula-

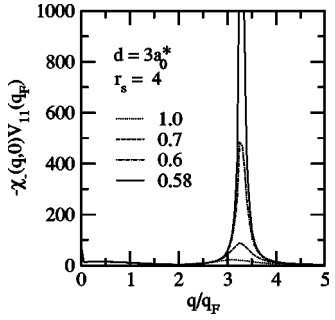


FIG. 9. Out-of-phase component of the static density susceptibility $\chi_-(q,0)$ for the coupled e-e wire system for different $b/a_0^*$ at indicated $r_s$ and $d/a_0^*$; legends indicate the values of $b/a_0^*$.

tions, although for a cylindrical quantum wire model of Gold and Ghazali,[27] also predict a reduction in critical $r_s$ for the formation of WC ground state, and interestingly, the reduction factor is of the same order as that predicted by the qSTLS theory.

The STLS approach again predicts transition only to a long-wavelength CDW ground state. A detailed account of the STLS results of $\chi_-(q,0)$ has been presented by one of the present authors in Ref. 16. The difference between the predictions of the qSTLS and STLS approaches arises once again due to a marked difference in the behavior of their respective LFCs as can be noticed from Figs. 10(a) and 10(b), where $G_{11}(q,0)$ and $G_{12}(q,0)$ are plotted as a function of $d$ at $r_s=4.8$ and $b/a_0^*=1$ along with the corresponding STLS LFCs. The $q$ dependence of $G_{11}(q,0)$ is like that in the

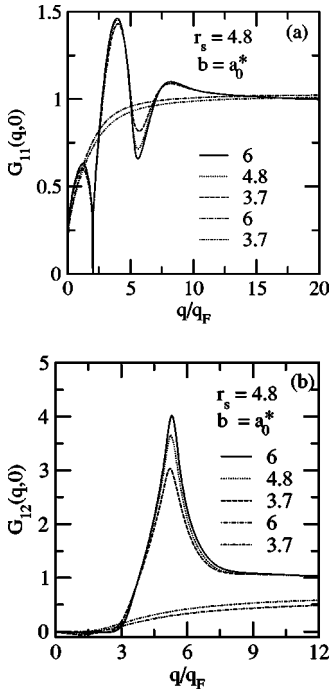


FIG. 10. Intrawire [in panel (a)] and interwire [in panel (b)] static local fields $G_{11}(q,0)$ and $G_{12}(q,0)$ for the coupled e-e wire system in the qSTLS approach at indicated $r_s$, $b$, and $d$. The STLS local fields are shown for comparison at $d/a_0^*=6$ and 3.7. Legends indicate the values of $d/a_0^*$.

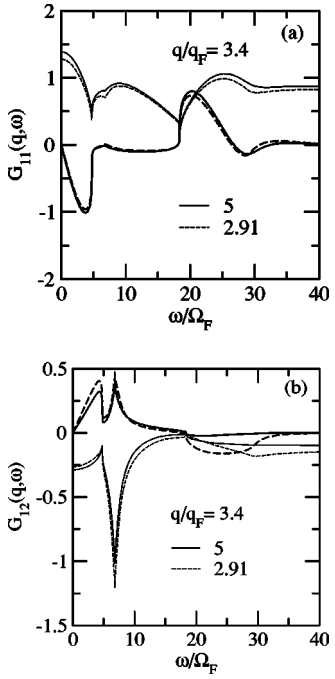


FIG. 11. Frequency dependence of intrawire [in panel (a)] and interwire [in panel (b)] local fields $G_{11}(q,\omega)$ and $G_{12}(q,\omega)$ for the coupled e-h wire system at $q/q_F=3.4$, $r_s=4.25$, $b/a_0^*=1$, and $d/a_0^*=5$ and 2.91. Thin and thick lines represent, respectively, the real and imaginary parts. Legends indicate the values of $d/a_0^*$, and $\Omega_F$ is the Fermi frequency.

e-h wire system, while $G_{12}(q,0)$ now has a strong positive peak at $q/q_F \approx 5.2$—the features which are completely absent in the STLS LFCs.

### D. Dynamic local fields

Finally, we examine the local fields for their dependence on frequency, as it may be useful to understand the reasons underlying the difference in predictions of the qSTLS and STLS approaches. The dynamic LFCs can be computed by using Eq. (3) once we have the self-consistent $S_{11}(q)$ and $S_{12}(q)$. We find quite generally that the real and imaginary parts of the intra- and interwire LFCs exhibit, both for the e-h and e-e wire systems, an oscillatory behavior as a function of real frequency $\omega$. In the large-$\omega$ limit, the respective real parts approach a frequency-independent value, while the imaginary parts become exactly equal to zero. This result is in conformity with the analytically obtained limiting results. The oscillatory character of the LFCs seems to be a basic feature of the qSTLS theory, as a qualitatively similar behavior has been observed for the 3D,[33] 2D,[18] 1D,[26] and bilayer systems.[19,20] Figures 11 and 12 contain, respectively, the results of dynamic LFCs for the e-h and e-e wire systems at $q/q_F=3.4$ at critical wire parameters associated with the formation of the WC ground state. A qualitatively similar behavior of LFCs is found at other values of $q$, and $r_s$, $b$, and $d$.

## IV. SUMMARY AND CONCLUDING REMARKS

In summary, we have studied the ground-state behavior of the coupled e-h and e-e quantum wire systems by including

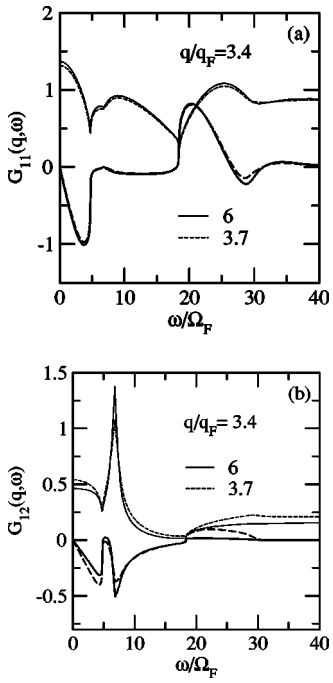


FIG. 12. (a), (b) Dynamic local fields for the coupled e-e wire system at indicated parameters; description of the curves is exactly the same as in Fig. 11 except for the fact that $r_s=4.8$.

the effect of dynamic correlations within the quantum version of Singwi, Tosi, Land, and Sjölander (qSTLS) theory. The importance of the dynamical character of correlations is highlighted by comparing our results with the predictions of the STLS approach, where correlations are treated at the static level. The comparative study explicitly reveals that the dynamics of correlations becomes increasingly important with the increasing dominance of the interaction effects over the kinetic effects. Their inclusion in the form of the qSTLS theory brings in both the quantitative and qualitative changes in the description of the many-body properties of the wire system. As an important distinctive result, the qSTLS theory predicts that the liquid phase, both in the e-h and e-e wire systems, can become unstable against a phase transition into a coupled WC ground state at sufficiently low particle density and/or narrow wire size in the close vicinity of two wires. Interestingly, the interwire correlations are found to reduce the critical $r_s$ for the onset of Wigner crystallization as compared to that for an isolated quantum wire system, and at $b/a_0^*=1$ the reduction in $r_s$ is about 15% and 4% for the e-h and e-e wire systems, respectively. Further, the value of critical $r_s$ is found to decrease with reduction in wire size. For $r_s$ lower than the critical $r_s$ for Wigner crystallization, but higher than a certain cutoff value, the qSTLS theory predicts a transition to a long-wavelength CDW ground state. Thus, a crossover seems to occur from a CDW ground state to a WC ground state. Our prediction of Wigner crystallization for the e-e wire system is found to be in qualitative agreement with the recent results of Tanatar,[32] which they have obtained on the basis of an approximate density functional theory calculation. It should be interesting to have similar calculations for the e-h wire system.

In our present work, we have focused mainly on the possible instability of the liquid phase, for the coupled e-e and e-h systems, against a transition into a charge density modulated phase. Other instabilities could also occur such as those associated with the spin density wave, and the partially and fully (the Stoner instability) spin-polarized phases.[34] It is important to mention here that although the Lieb-Matis[35] theorem rules out the spontaneous complete spin ordering in a strictly 1D electron system, there are recent experiments[36] supporting the formation of such a spin-ordered state at low density in low-disorder GaAs/GaAlAs-based electron quantum wire.

Although we have carried out our calculations of the ground-state properties for a specific quantum wire model, we believe that our conclusions should also apply (at the qualitative level) to other wire models. Finally, it may be mentioned here that to the best of our knowledge, unlike the 3D and 2D electron systems, no QMC simulation studies are available for the ground-state properties of both the single and double quantum wire systems. However, we anticipate that our present study may stimulate the QMC simulations of such quantum wire systems, which in turn would provide a benchmark to judge the accuracy of our present or of any other theoretical predictions. Apart from the QMC simulations, it should be interesting to have specific experimental studies aimed at exploring the possibility of the existence of the WC ground state in the quantum wire systems. For instance, one may look at examining the behavior of drag resistivity in these systems. The presence of a transition to the WC state, if any, should manifest as a divergence in drag resistivity. Very recently, Debray[37] have performed the drag resistance measurements for the coupled e-e wire system. It would be important to have these measurements in the low electron density region. The coupled e-h wire system would be a better choice for such experiments since the WC transition is expected to occur at relatively higher density (i.e., lower $r_s$) in this system due to the heavier effective mass of holes than electrons. On the theory side, the calculation of the Coulomb drag rate[38] in the coupled quantum wire system should be equally important for confirming the transition to the WC phase, and it deserves a separate, thorough investigation.

## ACKNOWLEDGMENTS

The authors gratefully acknowledge the financial support from the Department of Science and Technology, New Delhi.

*Electronic address: tankesh@pu.ac.in
†Electronic address: uccck@granth.kuk.ernet.in

[1] For review, see T. Ando, A. B. Fowler, and F. Stern, Rev. Mod. Phys. **54**, 437 (1982); A. Isihara, Solid State Phys. **42**, 271 (1989).
[2] For review, see C. W. J. Beenakker and H. van Houten, in *Solid State Physics: Semiconductor Heterostructures and Nanostructures* (Academic, Boston, 1991), Vol. 44.
[3] Y. W. Suen, L. W. Engel, M. B. Santos, M. Shayegan, and D. C. Tsui, Phys. Rev. Lett. **68**, 1379 (1992); J. P. Eisenstein, G. S. Boebinger, L. N. Pfeiffer, K. W. West, and S. He, *ibid.* **68**, 1383 (1992).
[4] H. C. Manoharan, Y. W. Suen, M. B. Santos, and M. Shayegan, Phys. Rev. Lett. **77**, 1813 (1996).
[5] L. Swierkowski, D. Neilson, and J. Szymanski, Phys. Rev. Lett. **67**, 240 (1991); D. Neilson, L. Swierkowski, J. Szymanski, and L. Liu, *ibid.* **71**, 4035 (1993); J. Szymanski, L. Swierkowski, and D. Neilson, Phys. Rev. B **50**, 11 002 (1994); L. Liu, L. Swierkowski, D. Neilson, and J. Szymanski, *ibid.* **53**, 7923 (1996).
[6] D. Lu, K. I. Golden, G. Kalman, P. Wyns, L. Miao, and X. L. Shi, Phys. Rev. B **54**, 11 457 (1996); and references cited therein; G. Kalman and K. I. Golden, *ibid.* **57**, 8834 (1998); G. Kalman, V. Valtchinov, and K. I. Golden, Phys. Rev. Lett. **82**, 3124 (1999).
[7] F. Rapisarda and G. Senatore, Aust. J. Phys. **49**, 161 (1996); in *Strongly Coupled Coulomb Systems*, edited by G. Kalman, J. M. Rommel, and K. Blagoev (Plenum Press, New York, 1998), p. 529; G. Senatore, F. Rapisarda, and S. Conti, Int. J. Mod. Phys. B **13**, 479 (1999).
[8] G. Goldoni and F. M. Peeters, Europhys. Lett. **37**, 293 (1997); **38**, 319 (1997).
[9] J. S. Thakur and D. Neilson, Phys. Rev. B **56**, 10 297 (1997).
[10] V. I. Valtchinov, G. Kalman, and K. B. Blagoev, Phys. Rev. E **56**, 4351 (1997).
[11] See, for instance, Q. P. Li and S. Das Sarma, Phys. Rev. B **43**, 11 768 (1991); B. Y.-K. Hu and S. Das Sarma, *ibid.* **48**, 5469 (1993); S. Das Sarma and E. H. Hwang, *ibid.* **54**, 1936 (1996), and references cited therein.
[12] A. Gold, Philos. Mag. Lett. **66**, 163 (1992).
[13] R. Wang and P. P. Ruden, Phys. Rev. B **52**, 7826 (1995).
[14] J. Hubbard, Proc. R. Soc. London, Ser. A **243**, 336 (1958).
[15] K. S. Singwi, M. P. Tosi, R. H. Land, and A. Sjölander, Phys. Rev. **176**, 589 (1968); K. S. Singwi and M. P. Tosi, Solid State Phys. **36**, 177 (1981).
[16] R. K. Moudgil, J. Phys.: Condens. Matter **12**, 1781 (2000).
[17] D. Neilson, L. Swierkowski, A. Sjölander, and J. Szymanski, Phys. Rev. B **44**, 6291 (1991).
[18] R. K. Moudgil, P. K. Ahluwalia, and K. N. Pathak, Phys. Rev. B **51**, 575 (1995); **52**, 11 945 (1995).
[19] R. K. Moudgil, L. K. Saini, and G. Senatore, Phys. Rev. B **66**, 205316 (2002).
[20] B. Tanatar and B. Davoudi, Phys. Rev. B **63**, 165328 (2001).
[21] B. Tanatar and D. M. Ceperley, Phys. Rev. B **39**, 5005 (1989).
[22] S. De Palo, F. Rapisarda, and G. Senatore, Phys. Rev. Lett. **88**, 206401 (2002).
[23] T. Hasegawa and M. Shimizu, J. Phys. Soc. Jpn. **38**, 965 (1975).
[24] N. Mutluay and B. Tanatar, Phys. Rev. B **55**, 6697 (1997).
[25] J. S. Thakur and D. Neilson, Phys. Rev. B **56**, 4671 (1997).
[26] B. Tanatar and C. Bulutay, Phys. Rev. B **59**, 15 019 (1999).
[27] See, for instance, A. Gold and A. Ghazali, Phys. Rev. B **41**, 7626 (1990); G. Y. Hu and R. F. O'Connell, *ibid.* **42**, 1290 (1990).
[28] F. Stern, Phys. Rev. Lett. **18**, 546 (1967).
[29] See, for example, G. D. Mahan, *Many-Particle Physics*, 2nd ed. (Plenum, New York, 1990).
[30] U. de Freitas, L. C. Ioriatti, and N. Studart, J. Phys. C **20**, 5983 (1987).
[31] J. S. Thakur, D. Neilson, and M. P. Das, Phys. Rev. B **57**, 1801 (1998), and references cited therein.
[32] B. Tanatar, I. Al-Hayek, and M. Tomak, Phys. Rev. B **58**, 9886 (1998).
[33] A. Holas and S. Rahman, Phys. Rev. B **35**, 2720 (1987).
[34] The recent QMC simulations have predicted that there occurs in the liquid phase a continuous (an abrupt) spin-polarization phase transition in a 3D (2D) electron system at relatively low electron density. For 3D, see G. Oritz, M. Harris, and P. Ballone, Phys. Rev. Lett. **82**, 5317 (1999), and for 2D see C. Attaccalite, S. Moroni, P. Gori-Giorgi, and G. B. Bachelet, *ibid.* **88**, 256601 (2002).
[35] E. H. Lieb and D. Mattis, Phys. Rev. **125**, 164 (1962).
[36] K. J. Thomas *et al.*, Phys. Rev. Lett. **77**, 135 (1996); K. J. Thomas *et al.*, Phys. Rev. B **61**, R13 365 (2000); D. J. Reilly *et al.*, Phys. Rev. Lett. **89**, 246801 (2002).
[37] P. Debray *et al.*, J. Phys.: Condens. Matter **13**, 3389 (2001); P. Debray *et al.*, Semicond. Sci. Technol. **17**, R21 (2002).
[38] B. Tanatar, Phys. Rev. B **58**, 1154 (1998), and references cited therein.